83-GT-9

THE AMERICAN SOCIETY OF MECHANICAL ENGINEERS
345 E. 47 St., New York, N.Y. 10017

ON THE INFLUENCE OF THE DIFFUSER INLET SHAPE ON THE PERFORMANCE OF A CENTRIFUGAL COMPRESSOR STAGE

K. Bammert
Professor Emeritus

M. Jansen
Chief Engineer

M. Rautenberg
Professor

all University of Hannover
Hannover, West Germany

ABSTRACT

Results from an experimental study of the influence of the diffuser inlet shape on the performance of the diffuser and the whole compressor stage are presented. The investigations were carried out using a single stage centrifugal compressor. Three different vaned diffusers were tested. From detailed flow field measurements the influence of the diffuser inlet shape on the performance of the essential components of the compressor stage, i.e. the impeller, the diffuser, and the collecting chamber was analyzed. It is shown that the reaction of the vaned diffuser on the efficiency of the impeller is only weak but the losses in the collecting chamber are considerably affected by the used diffuser types.

NOMENCLATURE

AR	area ratio, h_6/h_5
AS	aspect ratio of diffuser throat, b_5/h_5
A_{eff}	cross section calculated by continuity equation, m^2
A_{geo}	geometrical cross section, m^2
B	throat blockage, $1-A_{eff}/A_{geo}$
b	diffuser width, m
c	absolute velocity, m/s
c_p	diffuser recovery
d	diameter, m
h	enthalpy, kJ/kg or height of the diffuser throat, m
l	length of the diffuser channel, m
M	Mach number
$\dot{m}$	mass flow rate, kg/s
n	rotational speed, rpm
n	polytropic coefficient
p	pressure, bar
q	dynamic head, bar
r	radius, m
r_N	radius of the leading edge, mm
Δ R	friction loss, kJ/kg
s	entropy, J/kgK
T	temperature, K
u	circumferential velocity, m/s
W	work input, kJ/kg
Z	number of vanes
z	axial coordinate, m
α	flow angle between absolute and circumferential velocity, deg
β	angle between diffuser vane and tangent plane, deg
Δ	difference
η	efficiency, percent
θ	diffuser channel angle, $\arctg((h_6-h_5)/2\,l)$, deg
$\varkappa$	isentropic exponent
λ	diffuser radius ratio, r/r_2
π	pressure ratio, p/p_K
τ	temperature ratio, T/T_K

Subscripts

K	stagnation condition in the equalizing chamber
r	radial
R	extra work for compressing the heated fluid
S	collecting chamber (compressor outlet)
s	isentropic

SR	static loss due to friction
tot	total
u	circumferential
v	loss
1	entrance; inlet area
2	impeller exit; outlet area
4	diffuser inlet
5	diffuser throat
6	diffuser exit
7	pressure pipe

Superscripts

*	related value
-	mean value

INTRODUCTION

It was the aim of centrifugal compressor development to achieve larger volume rates of flow and higher stage pressure ratios and in particular to use the input energy more effectively, i.e. to reduce the losses in the flow passages in the centrifugal compressor. Fig. 1 shows a simplified sectional view of a single-stage centrifugal compressor. The flow passages in such a compressor can be subdivided into three sections. The impeller is arranged between planes I and II, the diffuser between planes II and III and the discharge collecting chamber between planes III and IV. Special attention must be paid to the diffuser in respect of loss occurrence. It is important to adapt the diffuser to the impeller exit flow to obtain the best possible energy transformation within the diffuser. However, during the design stage a diffuser should never be regarded as an isolated component but as one which has to function together with other components of the stage.

Compressors featuring high stage pressure ratios are predominantly equipped with vaned diffusers. However, there are still uncertainties in the design of the vaned diffusers for centrifugal compressors. Theoretical and experimental investigations in a diffuser are very expensive because the flow is non-steady especially in the diffuser inlet region and flow separation must be expected even if twisted vanes are used. Flow mechanisms, in particular in the inlet region of vaned diffusers, and interactions within the inlet, impeller, diffuser, and compressor outlet system are clear only in part.

It is the objective of the present investigation to find a suitable method of influencing the procedure of a compressor diffuser, which works within a relatively narrow operating range, by using a suitable diffuser vane design and to find the influence which the inlet geometry of the diffuser exerts on the other components of the compressor stage. A radial compressor with a 90 degree impeller and three differently vaned diffusers were chosen for the investigations. Two of the diffusers were of conventional design featuring constant inlet flow angle across the width. The third diffuser had been specially adapted to the angle distribution of the impeller outlet flow, which resulted in a three-dimensionally twisted diffuser vane shape. All three diffusers were investigated in conjunction with the same impeller and the same discharge collecting chamber. Care was taken to ensure that the working principles of both the diffusers and the other components of the compressor could be assessed.

The performance maps of the compressor with the three different vaned diffusers and some characteristic traverse data for the twisted diffuser were presented in (1)[1]. In this paper the influence of the diffuser inlet shape on the performance of the essential components of the compressor stage, the impeller, the diffuser and the collecting chamber is analysed.

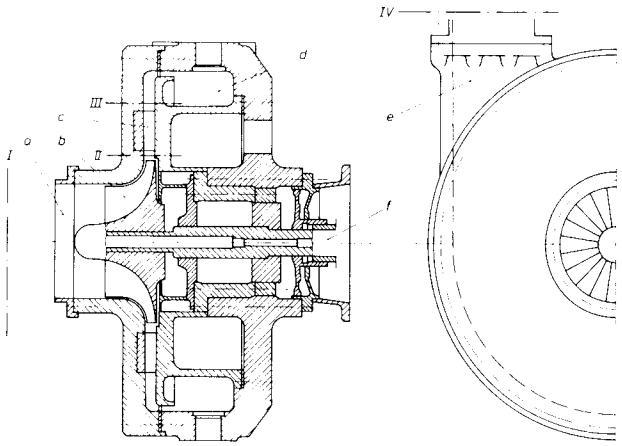

Fig. 1 Simplified sectional view of the compressor

a inlet	d collecting chamber
b impeller	e pressure pipe
c diffuser	f drive

I - IV measuring sections

DEFINITIONS OF LOSS AND EFFICIENCY

Suitable definitions of loss and efficiency are indispensable to permit an assessment of the performance of the entire compressor stage, the losses in each component of the stage and in each diffuser in respect of their energy transformation. The compressor and its components under consideration are regarded as adiabatic continuous flow systems. An assessment of the entire compressor stage makes it imperative to calculate the energy balance of the process of compression. Fig. 2 shows the adiabatic frictional compression in the h,s-diagram. Indices 1 and 2 stand for the inlet and outlet areas of the system. The work W_{12} supplied through the compressor shaft equals the increase in the static enthalpy Δh and the change in the energy of velocity

$$W_{12} = \Delta h + \frac{c_2^2}{2} - \frac{c_1^2}{2} \quad . \qquad (1)$$

1 Numbers in parentheses designate references at end of paper.

The ratio of the work input of an ideal machine Δh_{tots} to that of a real machine Δh_{tot} is to be used for an assessment of the working principle of the entire compressor stage. This ratio is called the efficiency of the stage

$$\eta = \frac{\Delta h_{tot\,s}}{\Delta h_{tot}} = \frac{\pi_{tot}^{\frac{\varkappa-1}{\varkappa}} - 1}{\tau_{tot} - 1} \quad . \qquad (2)$$

The kinetic energy at the compressor outlet is not regarded as loss. The additional work of the real machine over that of the ideal machine in the h,s-diagram, expressed by the difference in enthalpies $\Delta h_v = \Delta h - \Delta h_s$, is composed of the friction losses ΔR and the additional work W_R necessary for the compression of the medium heated up by friction losses, namely

$$\Delta h_v = \Delta R + W_R \quad . \qquad (3)$$

In an adiabatic system, the heat ΔR produced by friction and included in the medium handled, is calculated in accordance with the second principal theorem of thermodynamics, namely

$$\Delta R = \int_1^2 T \cdot ds \quad , \qquad (4)$$

The friction losses caused in each component are to be used and the additional work is to be regarded as useful work in connection with the assessment of the components of a compressor stage and their interrelations. When comparing identical components - but different loss variants - it is convenient to relate the friction losses to the increase in the static enthalpy in the component concerned (2) . The following definition of the static loss efficiency is derived therefrom:

$$\eta_{SR} = 1 - \frac{\Delta R}{\Delta h} \quad . \qquad (5)$$

This efficiency allows for all friction losses which occur in the flow of the medium. It is to be assumed in the following considerations that η_{SR} remains constant along the change of condition under consideration. The following equation results for the static loss efficiency for such a polytropic change in condition:

$$\eta_{SR} = \frac{n}{n-1} \cdot \frac{\varkappa-1}{\varkappa} \qquad (6)$$

with the following polytropic exponent:

$$n = \frac{\ln \pi}{\ln \left(\frac{\pi}{\tau}\right)} \quad . \qquad (7)$$

However, the judgement of the performance of a diffuser cannot only be based on the losses which occur because they give little information about the energy transformation in the diffuser. The degree of pressure transformation

$$c_P = \frac{p_2 - p_1}{q_1} \qquad (8)$$

and the dynamic pressure

$$q_1 = \frac{\varkappa}{\varkappa-1} \cdot p_1 \cdot \left[\left(\frac{p_{tot\,1}}{p_1}\right)^{\frac{\varkappa-1}{\varkappa}} - 1\right] \qquad (9)$$

must therefore be included in our considerations. The above degree of transformation expresses the relationship between the actual static pressure rise and the ideal static pressure rise and is always smaller than unity because the exit velocity must be different from zero.

To permit comparable efficiencies, characteristic numbers and flow values to be calculated or measured directly for various inlet conditions, the speed and the mass flow are so adjusted that both rated to standard condition remain constant. The standard condition means p = 1.01325 bar and T = 288.15 K.

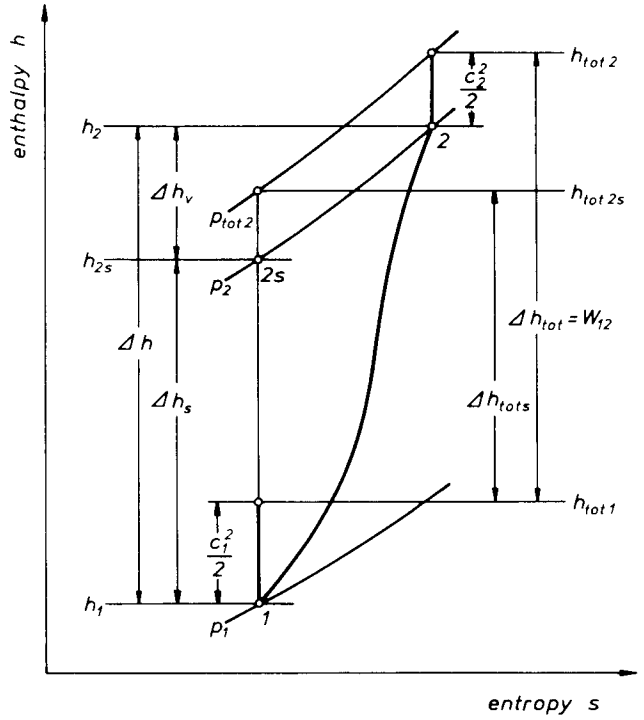

Fig. 2 Adiabatic, irreversible compression process

TEST RIG

The investigations were carried out on a test rig, which is described in detail in (3). The flow areas in the test compressor are relatively large so that the requisite measurements with probes in the diffuser did not pose any problems. Several diffusers were designed and investigated for this test rig (1, 4), namely

a cambered vane diffuser with aerodynamic shaped cascade,

a straight channel diffuser with vertical flanking blade position, and

a twisted diffuser adapted to the inlet flow.

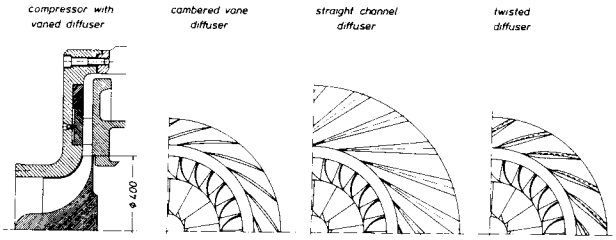

Fig. 3 Compressor with the tested vaned diffusers

Diffuser installation in the radial compressor was as is shown in Fig. 3. The compressor map point defined by a speed n = 22,000 rpm and a mass flow rate $\dot{m}$ = 8.59 kg/s was used as the design point for all three diffusers. The design was based on the flow measurements effected in the compressor equipped with a vaneless constant-area diffuser (5). Table 1 contains the characteristic design data of all three diffusers. All important symbols can be seen in the left-hand column. Index 4 refers to the diffuser inlet.

$\dot{m}$ means mass flow, π_4 is the static pressure ratio, $\pi_{tot,4}$ the total pressure ratio, $\tau_{tot,4}$ the total temperature ratio, M_4 the local Mach number and α_4 the flow angle. The design of the cambered vane diffuser and of the straight channel diffuser was based

Table 1 Characteristics of the vaned diffusers

symbol	dim.	cambered vane diffuser	straight channel diffuser	twisted diffuser		
				z/b 1/6	3/6	5/6
$\dot{m}$	kg/s	8.59	8.59	1.30	2.80	4.49
π_4	-	2.693	2.794	2.704	2.704	2.704
$\pi_{tot,4}$	-	4.716	4.769	4.674	4.888	5.303
$\tau_{tot,4}$	-	1.70	1.70	1.71	1.71	1.71
M_4	-	0.93	0.91	0.92	0.96	1.03
α_4	deg	16.9	16.5	8.8	18.5	28.2
Z	-	19	19	19		
λ_4	-	1.15	1.15	1.15		
λ_6	-	1.50	1.95	1.55		
b_4/r_2	-	0.119	0.119	0.119		
β_4	deg	16.9	17.8	4/33 +		
β_6	deg	26.9	55.8	37		
r_N	mm	0.2	0.5	0.2		
2Θ	deg	7.3	9	8.8		
AR	-	1.58	2.15	1.98		
l/h_5	-	5.13	7.04	4.06		
AS	-	0.90	0.86	0.79		
B	-	0.13	0.1	0.09		

+ front wall / back wall

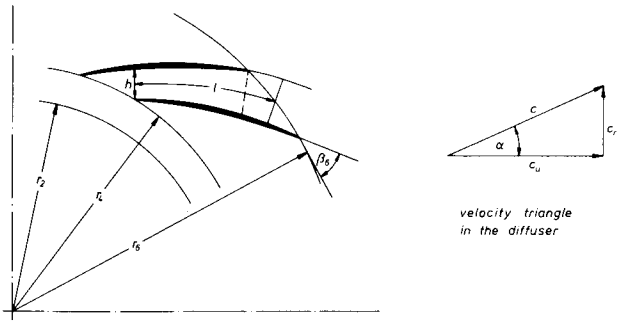

Fig. 4 Diffuser geometry and velocity triangle

on such values of the individual flow parameters as had been averaged using the inlet cross-sectional areas and different principles. For the purpose of its design, the cambered vane diffuser was regarded as a radial cascade whilst the straight channel diffuser was treated as an arrangement of single channels (6). Both design principles led to two-dimensional diffuser geometries with constant vane incidence angles over the diffuser width. In the design of the twisted diffuser, the distribution of flow parameters over the diffuser width was taken into account. A linear progression of the angle α_4 over the diffuser width was assumed. The design was based on a one-dimensional flow calculation made for several planes of the diffuser width (7). Therefore, table 1 shows the values of three diffuser width ratios z/b for the twisted type. Characteristic diffuser figures are then shown in the left-hand column, namely the number of diffuser vanes Z, the radius ratios λ_4 and λ_6 on which the diffuser inlet and outlet radii run, the diffuser width b_4 related to the impeller exit radius r_2, angles β_4 and β_6 of the mean camber lines at the diffuser inlet and outlet, and radius r_N of the vane leading edge. Moreover, the same column contains the diffuser channel angle 2θ, the area ratio AR, the length ratio l/h_5 (where l is the length of the diffuser channel and h_5 the height of the diffuser channel as measured at its inlet), the aspect ratio AS, and the throat blockage B upon which the design is based. Fig. 4 illustrates the principal geometrical values and the velocity triangle in the diffuser. Common to all three diffuser types was that they had 19 vanes and began with a diffuser radius ratio of λ = 1.15. The vaneless region between the impeller and the diffuser was a convergent constant-area diffuser, and the sidewalls of the vanes part were parallel.

TEST RESULTS

Compressor maps were plotted to permit an assessment of the influence of the diffusers investigated on the working principle of the total compressor. These maps were related to the thermodynamic condition in the inlet chamber and the pressure pipe (a and e Fig.1). Flow measurements were made before and after the diffuser to obtain information about the working of each component, namely impeller, diffuser, and compressor outlet, and information about the influence of non-uniform inlet flow on the pressure build-up in the diffuser. Using various types of probes, the total pressure, the total temperature and the flow angle were measured. Scanning was carried out before the blading at λ = 1.1 and after the diffuser blades at λ = 1.6, at several points over the diffuser pitch and the diffuser width.

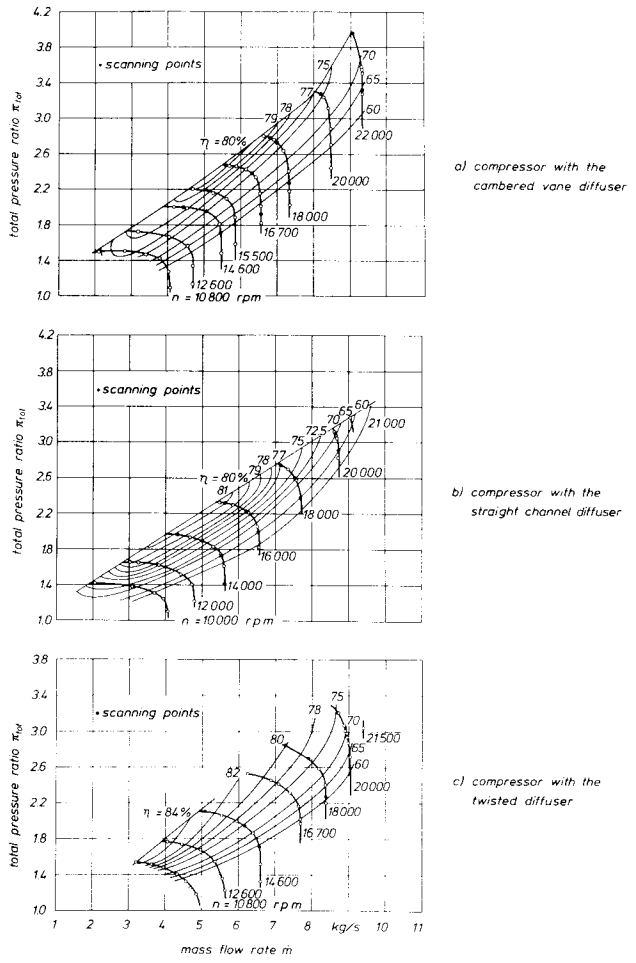

Fig. 5 Compressor maps

INFLUENCE OF THE DIFFUSERS ON THE PERFORMANCE OF THE COMPRESSOR STAGE

Fig. 5 shows the performance maps of the compressor equipped with a cambered vane diffuser (Fig. 5a), a straight channel diffuser (Fig. 5b) and a twisted diffuser (Fig. 5c). The total pressure ratio π_{tot} is shown in each case versus the mass flow rate $\dot{m}$. Moreover, the diagrams contain lines of constant efficiency η. The characteristic lines were run from choke flow to surge limit. The surge limit was not directly approached for speeds over n = 14,600 rpm in the case of the twisted diffuser. The capacity limit of the compressor was reached here at speeds over 20,000 rpm. The centre of the efficiency shell curves lies immediately at the surge limit line for all three compressor variants.

It is noted when comparing the three performance maps that the map of the compressor equipped with a twisted diffuser is shifted towards higher mass flow rates as compared with the cambered vane and the straight channel diffuser, in particular in the low speed range. The optimum efficiency of the compressor equipped with a twisted diffuser is in a somewhat lower speed range as compared with the two other compressor variants. However, mention must be made of the fact that the twisted diffuser generally reaches better efficiencies. The improvement in efficiency in the lower speed range is higher than 4 % as compared with the compressor with the cambered vane diffuser and another 3 % as compared with the straight channel diffuser. In the upper speed range, the compressor with its twisted diffuser shows a clearly wider operating range. The characteristic field width at n = 18,000 rpm is more than twice as wide as that of the compressor with cambered vane and straight channel diffuser.

DISTRIBUTION OF TOTAL LOSSES TO THE COMPONENTS OF THE COMPRESSOR STAGE

A comparison of the performance maps revealed that the compressor equipped with the twisted diffuser showed better efficiencies and a clearly wider operating range. To permit an assessment of the performance of each diffuser and its influence on the working of the other components of the compressor stage, the total losses of the compressor are distributed to the individual components. Three systems (componets) are considered for this purpose, namely

the impeller with its inlet and the impulse compensation zone which follows immediately after the impeller outlet,

the vaned diffuser with its heavy reaction region upstream of the throat, and

the compressor outlet.

The compressor outlet consists of a transition between the vaned diffuser and the discharge collecting chamber, the collecting chamber and the pressure pipe. The system delineations of the three components were the intake chamber, the concentric flow cross-sections in the diffuser with the diffuser radii ratios of λ = 1.1 and 1.6, and the measuring plane after the compressor in the pressure pipe. Fig. 1 shows these delineations I to IV.

This subdivision precisely encloses the vaned diffuser. The delineation at λ = 1.6 runs in the diffuser channel in the case of the straight channel diffuser. It was impossible to take measurements immediately after the straight channel diffuser because the flow is diverted there immediately into the discharge collecting chamber. The build-up of the pressure is finished at λ = 1.6, as is shown by the pressure distribution in the diffuser (7). Therefore, the system delineations cover the losses caused by the transformation of energy in the straight channel diffuser quite well. The losses which are caused at the diffuser outlet, in particular by the sudden widening of the flow area after the wedge-shaped blades, are attributed to the compressor outlet. The impulse compensation zone might be regarded as an independent area in respect of losses. These losses are hardly determined by the diffuser but chiefly by the flow in the impeller. For an assessment of the working principle of the impeller in conjunction with the various vaned diffusers it appears therefore convenient to attribute the losses to the impeller, especially as the contour of the vaneless diffuser did not change in that region. Since the inlet is only a short straight inlet nozzle, the losses caused there are low and are negligeable in the evaluation of the impeller wheel losses.

Representative average values of the thermodynamic condition of the flow during its passage through the test regions were determined to permit a calculation of the losses. The representation of the losses, effi-

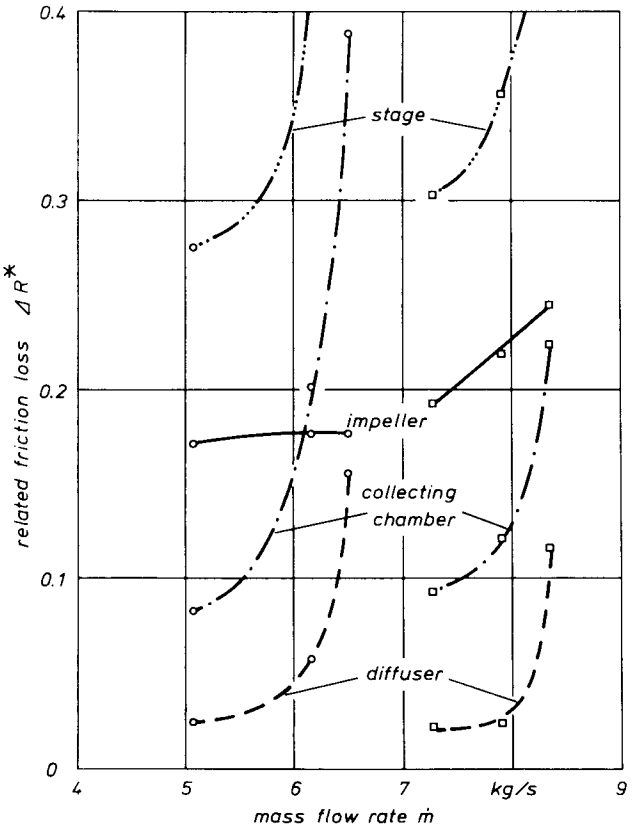

Fig. 6 Loss distribution in the compressor with the twisted diffuser

o n = 14,600 rpm ▫ n = 18,000 rpm

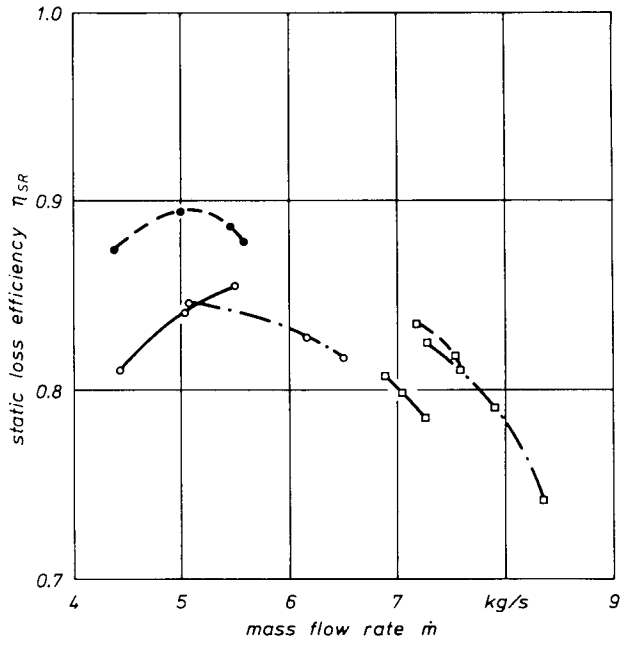

Fig. 7 Static loss efficiency of the impeller

—— cambered vane diffuser • n = 14,000 rpm
— — straight channel diffuser o n = 14,600 rpm
—·— twisted diffuser ▫ n = 18,000 rpm

ciencies and degrees of pressure conversion is limited in this connection to the results of the operating points of two characteristic speed curves for each compressor variant. The n = 14,600 rpm and 18,000 rpm speed curves were selected for the compressor with the cambered vane and the twisted diffuser. In the compressor equipped with the straight channel diffuser, measurements were not taken at n = 14,600 rpm but at n = 14,000 rpm, as in the case of the vaneless diffuser compressor. The distribution of total losses to the three components is qualitatively similar in the cases investigated. Therefore only one example is explained below.

Fig. 6 shows the related friction losses

$$\Delta R^* = \Delta R / (u_2^2 / 2) \qquad (10)$$

of the indivudual components of the twisted diffuser compressor versus the mass flow rate. u_2 is the circumferential velocity of the impeller at its outlet and ΔR is the friction loss. For clarity, values of $\Delta R^* < 0.4$ are only shown. When considering this friction loss, it must be noted that the compressor cannot be regarded as a strictly adiabatic system in the regions of the diffuser and the compressor outlet. For the comparisons made here of the results obtained from the same test rig, this influence can be neglected.

The distribution of the related friction losses reveals that the losses in the diffuser for operating points at the surge limit are much lower than those caused in the compressor outlet and in the impeller. In view of the fact that the compressor outlet should not take part in the transformation of energy, the losses caused in the outlet are rather high as compared with those of the two other components. In the choke flow vicinity the losses increase significantly both in the diffuser and in the compressor outlet. These high losses in the diffuser for operating points at the choke limit can be explained by the occurrence of supersonic areas and flow separations in the diffuser channel. The jet flow then leaving the diffuser causes high losses in the compressor outlet, too. The nearly parallel shape of the curves of the friction losses of the diffuser and the compressor outlet shows that a disturbance of the flow in the region of the vaned diffuser influences the losses in that component and directly also those in the compressor outlet.

INFLUENCE OF DIFFUSERS ON THE WORKING PRINCIPLE OF THE COMPONENTS

The static loss efficiency is calculated for the impeller in accordance with (7) to permit an assessment of the influence of the vaned diffuser on the working principle of the impeller. Fig. 7 illustrates the progression of the static loss efficiency of the impeller versus the mass flow rate for the characteristic curves selected and for different diffuser combinations. The efficiency curves run within a relatively wide band, which falls as the speed increases. The efficiencies increase up to a mass flow rate of $\dot{m} \approx 5$ kg/s and then decrease as the mass flow rate increases. The efficiency curve of the impeller combined with the

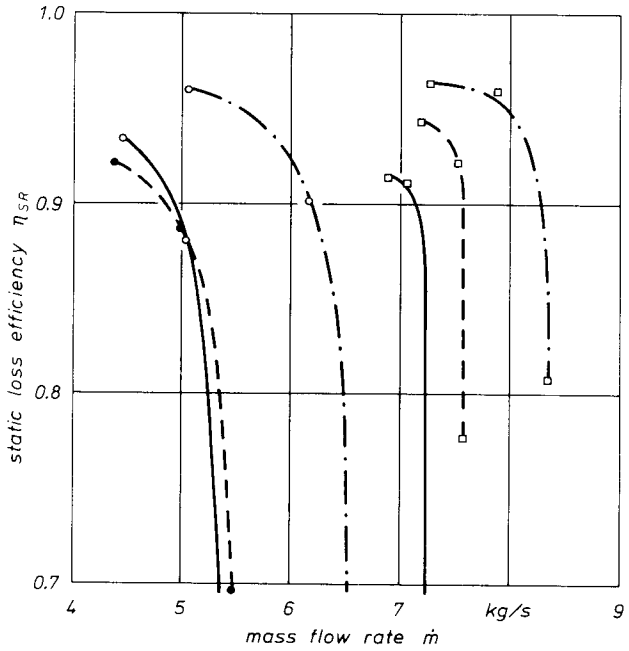

Fig. 8 Static loss efficiency of the diffuser

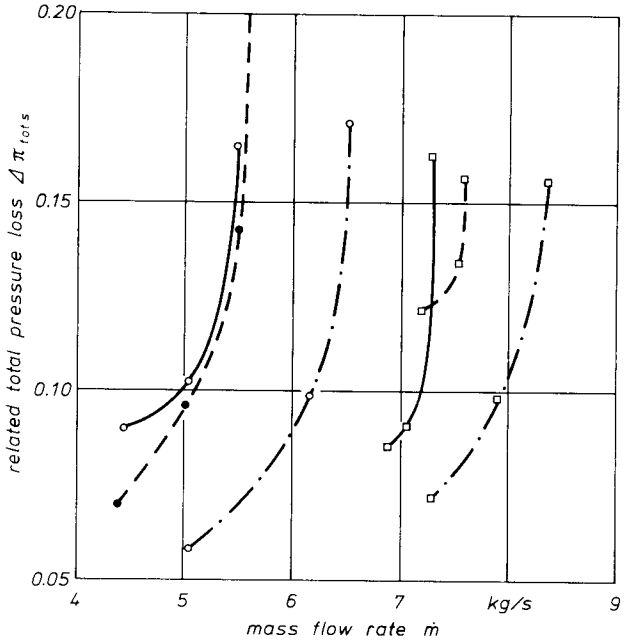

Fig. 9 Total loss in the compressor outlet

——— cambered vane diffuser ● n = 14,000 rpm
— — straight channel diffuser o n = 14,600 rpm
—·— twisted diffuser □ n = 18,000 rpm

straight channel diffuser is for n = 14,000 rpm clearly higher than those of the impeller with the two other diffusers at n = 14,600 rpm. This is partly explained by the low number of revolutions. The efficiency curves of the impeller equipped with the twisted diffuser and the straight channel diffuser are nearly congruent at n = 18,000 rpm whilst the efficiencies of the impeller equipped with the cambered vane diffuser are clearly worse. The steep fall of the efficiency of the impeller for compressor operating points at n = 18,000 rpm in the choke flow region suggests local supersonic areas and corresponding losses in the impeller.

There is certainly not any excessive rotroaction of the diffuser blading on the flow in the impeller. A possible retroaction of the heavy flow disturbances in the diffuser channel on the flow in the impeller, visible in the operating points at the choke flow limit, is blocked in the upstream direction by the simultaneous occurrence of supersonic phenomena in the diffuser throat. It can be seen that the impeller works more favourably in the lower speed range if equipped with the straight channel diffuser than with the two other diffusers. The impeller shows its optimum efficiency if equipped with the twisted diffuser or the straight channel diffuser at speeds around n = 18,000 rpm. The overall work of the impeller is no longer satisfactory in that speed range nor at high mass flows.

The working of the individual diffusers in the compressor is also assessed with the help of the static loss efficiencies. Fig. 8 illustrates the static loss efficiencies of the diffusers for the speeds selected, as a function of the mass flow rates. It can be seen that significantly better efficiencies are obtained with the twisted diffuser in both speed ranges.

The shape of the efficiency curves of the cambered vane and straight channel diffusers at low speeds makes us expect that these diffusers might show better efficiencies than the values given here for mass flow rates lower than those measured at the surge limit. A fundamental change in the statements made about the working principle of the diffusers is improbable in view of the shape of the efficiency curves even with comparable mass flow rates. Therefore, it can be said that the twisted diffuser produces lower losses than the two other diffusers, especially at high inlet Mach numbers.

The definition of the static loss efficiency is less advantageous for the purpose of comparing the working principles of the compressor outlet in conjunction with the three diffusers. The increase in static enthalpy in that component is small. Since this term is in the denominator of the equation, small measuring errors in the determination of the temperature are felt disproportionately much. The compressor outlet chiefly serves as a transition of the compressed medium to the connected piping. It is customary to characterize the working principle of a component used for flow guidance only by indicating the pressure drop which occurs. Therefore, the related total pressure loss

$$\Delta \pi_{tot\,S} = 1 - \bar{p}_{tot\,7} / \bar{p}_{tot\,\lambda=1.6} \qquad (11)$$

is employed for comparison, where index S refers to the compressor outlet, which is mainly formed by the discharge collecting chamber.

Fig. 9 shows the total pressure loss in the compressor outlet. Values as occur in operating points near

the surge limit of the compressor are plotted. The twisted diffuser causes fewer pressure losses than the two other diffusers. The more effective working of the compressor outlet in conjunction with the twisted diffuser is with certainty decisively influenced by the angle of diffuser outlet flow and consequently the selected blade outlet angle.

Fig. 10 illustrates the decrease of pressure transformation in the diffusers. The twisted diffuser and the straight channel diffuser achieve clearly better degrees of pressure transformation than the cambered vane diffuser. The latter diffuser would achieve better degrees of transformation in operating points with n = 18,000 rpm and lower mass flow rates but these efficiencies would nevertheless be clearly lower than those of the other two diffusers in view of the shape of the c_p curve plotted. The difference in the degree of pressure transformation between the cambered vane diffuser and the two other diffusers is mainly due to the smaller diffuser channel angle or the lower area ratio of the cambered vane diffuser (see table 1).

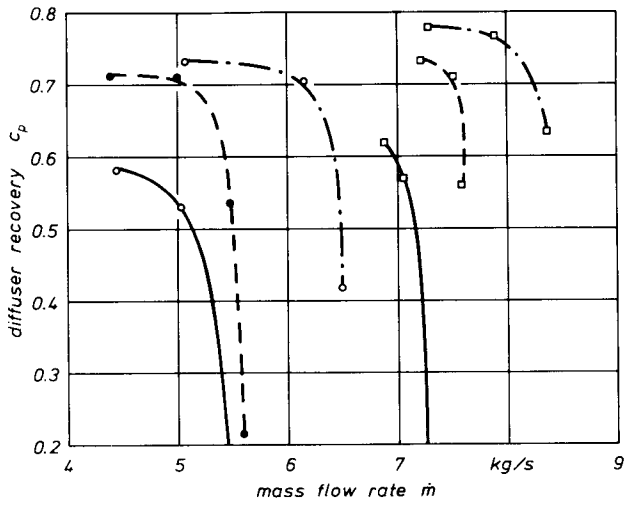

Fig. 10 Diffuser recovery

——cambered vane diffuser ● n = 14,000 rpm
— —straight channel diffuser o n = 14,600 rpm
—·—twisted diffuser □ n = 18,000 rpm

SUMMARY

Three vaned diffusers were investigated in a highly loaded centrifugal compressor. The design point and the aerodynamic marginal conditions of the diffusers were identical. However, the diffusers differed clearly in their geometries. Important parameters, such as the distribution of the vane inlet and outlet angles of the diffuser width and the effective inlet and outlet cross-sectional areas of the diffuser channels were changed in the diffusers tested. Moreover, the cross-sectional areas of flow in the twisted diffuser were not rectangular, contrary to the other diffusers.

The influence of the diffuser shapes on the working of the components of the compressor stage had to be assessed. Detailed flow measurements were made for this purpose.

The investigation results show that the compressor equipped with the twisted diffuser achieves better efficiencies and higher total pressure ratios. The operating range for total pressure ratios $\pi_{tot} > 2$ is clearly wider than that of the compressor equipped with the conventionally designed diffusers. The distribution of the total losses to the various components of the compressor stage revealed that pressure losses in the twisted diffuser were significantly lower than in the two other diffusers. No special effect of the twisted diffuser on the losses in the impeller was noticed. However, minor pressure losses occurred in the compressor outlet if the twisted diffuser was used. Using the decrease of pressure transformation it was shown that the twisted diffuser also allows a more efficient transformation of the kinetic energy.

REFERENCES

1 Jansen, M., M. Rautenberg, "Design and Investigations of a Three Dimensionally Twisted Diffuser for Centrifugal Compressors", ASME-Paper No. 82-GT-102, 1982.

2 Bammert, K., and M. Rautenberg, "Zur Ähnlichkeitsmechanik von Turboverdichtern," Wärme, Vol. 74, No. 1/2, 1968, pp. 37 - 51.

3 Bammert, K., M. Rautenberg, "On the Energy Transfer in Centrifugal Compressors", ASME-Paper No. 74-GT-121, 1974.

4 Bammert, K., M. Jansen, P. Knapp, W. Wittekindt, "Strömungsuntersuchungen an beschaufelten Diffusoren für Radialverdichter", Konstruktion 28, 1976, pp. 313 - 319.

5 Bammert, K., "Instationäre Strömungsmessungen vor dem Laufrad, längs der Laufradaußenkontur und nach dem Laufrad eines Radialverdichters", Forschungsvereinigung Verbrennungskraftmaschinen, Heft Nr. R 2o1, pp 1 - 26.

6 Bammert, K., "Experimentelle Untersuchungen an beschaufelten Diffusoren für hochbelastete Radialverdichter", Forschungsvereinigung Verbrennungskraftmaschinen, Heft Nr. R 278, pp. 1 - 46.

7 Jansen, M. "Untersuchungen an beschaufelten Diffusoren eines hochbelasteten Radialverdichters", Diss. University of Hannover, 1982.